Engineered Science
DOI: https://dx.doi.org/10.30919/es1249

Shear Strength of Stirrup-Free Recycled Aggregate Concrete Beams Reinforced with Steel Fibers

Satjapan Leelatanon,[1] Thanongsak Imjai,[1] Monthian Setkit,[1,*] Reyes Garcia[2] and Chau Khun Ma[3]

Abstract

The shear strength of recycled aggregate concrete (RAC) beams is usually lower than that of counterpart natural aggregate concrete (NAC) beams. The use of steel fibers can recover some of such shear strength, but research is needed to develop practical design tools for RAC beams reinforced with steel fibers. This article studies experimentally and analytically the shear strength of stirrup-free RAC beams reinforced with commercial steel fibers. Sixteen beams were tested in four-point bending using a shear-span-to-depth ratio (a/d) of 3.2. Fourteen of such beams were cast with RAC using 100% RCA reinforced internally with different fiber volume fractions (V_f = 0%, 0.5%, 0.75%, 1.0% or 1.5%), types of steel fibers (hook ends or double hook ends), and longitudinal reinforcement ratios (ρ_w = 1.6% and 2.5%). Another two control beams were cast with NAC without steel fibers. It was found that adding a minimum V_f = 0.5% of steel fibers to the RAC beams improved the shear strength by more than 51%. Steel fibers significantly improved shear behavior of RAC beams at volume fractions > 0.75% and prevented their shear failure. A shear stress limit of $0.3\sqrt{f_c'}$, as recommended by ACI 318-19 for normal beams with steel fibers used as shear reinforcement, can be conservatively adopted for the design of stirrup-free RAC beams with steel fibers. A new modification factor to the ACI 318-19 shear equation is also proposed to explicitly account for the effect of steel fibers and longitudinal reinforcement ratios on the shear strength of RAC beams. The findings in this article contribute towards the development of practical guidelines for the design of RAC elements with steel fibers subjected to high shear forces.

Keywords: Recycled concrete aggregate (RCA); Recycled aggregate concrete (RAC); Shear strength; Steel fibers; Fiber-reinforced concrete (FRC).
Received: 19 July 2024; Revised: 06 September 2024; Accepted: 29 September 2024.
Article type: Research article.

1. Introduction

Concrete is the primary material used in construction worldwide. However, concrete production and its subsequent end-of-life management pose a range of environmental challenges. These include cement production and its associated CO_2 emissions, high energy consumption, mining and extraction of raw materials, and waste generation after demolition at the end of service life of concrete structures. In recent years, numerous attempts have been made to reduce or replace the volumes of raw aggregates used in concrete. A potential solution is the replacement of natural aggregates with fine and coarse recycled concrete aggregates (RCA), which in turn can reduce the dependency on raw materials and decrease construction and demolition waste (CDW).[1]

The use of RCA obtained from CDW has been the main subject of research study for decades. Several works studied the mechanical properties and durability of RCA compared to natural aggregates.[2-7] The research findings suggest that the mechanical properties and durability of RCA are inferior to those of natural coarse aggregates (NCA). To improve the quality of RCA, several researchers[8-10] have proposed solutions to improve the quality of RCA. In spite of these, the resulting recycled aggregate concrete (RAC) produced with such RCA is often of lower quality than an equivalent natural aggregate concrete (NAC). As a result, RAC is frequently only used in non-structural applications in construction.

[1] *School of Engineering and Technology and Center of Excellence in Sustainable Disaster Management, Walailak University, Nakhon Si Thammarat 80160, Thailand.*
[2] *Civil Engineering Stream, School of Engineering, The University of Warwick, Coventry, CV4 7AL, United Kingdom.*
[3] *Forensic Engineering Centre, Institute for Smart Infrastructure and Innovative Construction, Faculty of Civil Engineering, Universiti Teknologi Malaysia, Skudai, Johor Bahru, 81310, Malaysia.*
**Email:* smonthia@wu.ac.th (M. Setkit)

Several researchers have studied the shear strength of reinforced RAC beams and slabs made with RAC and compared results to those from NAC specimens.[11-37] In some of these studies, the shear strength of RAC beams (with or without internal stirrups) was investigated by varying several parameters, such as the volume of RCA substitution, compressive strength of concrete, shear-span-to-depth ratio, longitudinal reinforcement ratio, and effective depth. The results from these experiments indicate that the shear strength of RAC beams decreased as higher volumes of RCA were used in the RAC. It was also found that the crack patterns of RAC beams were similar to those of counterpart NAC beams. Moreover, an increase in the shear-span-to-depth ratios reduced the shear strength of RAC beams. The shear strength of RAC beams was also lower in RAC beams with low longitudinal reinforcement ratios. In spite of this, it was also found that the shear strength of RAC beams could be conservatively predicted with the existing shear equations[20] included in ACI 318.[38]

A potential solution to enhance the shear strength of RAC is the use of fibers into the concrete mix. Several types of fibers (such as polypropylene and steel fibers) have been used to improve the mechanical properties of concrete and the flexural and shear strength of RC beams.[39-46] Particularly, steel fiber-reinforced concrete (SFRC) can offer enhanced tensile strength and crack control through the inclusion of steel fibers. Past studies have adopted different detailed techniques (e.g. piezoelectric transducers) to examine cracking and detect damage considering the fracture characteristics of the microstructure of SFRC.[47,48] The results indicate that the randomly distributed fibers in SFRC play a crucial role in crack propagation. The main parameters that affect this process include the fiber volume fraction, fiber aspect ratio, fiber orientation, as well as the maximum pullout stress (or debonding process) between fibers and the concrete matrix.[49] Moreover, the crack-bridging effect provided by the steel fibers significantly enhances the shear resistance of concrete, providing a pseudo-ductile response that contrasts with the brittle behavior of plain concrete subjected to shear forces. This in turn improves the residual strength of SFRC elements (especially in tension) and increases their energy dissipation capacities.[50] Adding fibers into concrete also enhances its toughness and durability. As a result, steel fibers are a promising alternative reinforcement in concrete elements subjected to shear forces[51] due to the good cracking performance of SFRC and, under specific circumstances, the brittle shear failure of elements can be changed to ductile (flexural dominated) failures.[52] The combination of RAC with steel fibers can lead to more sustainable and durable construction materials. Whilst a relatively large database of NAC beams with steel fibers exists [53] and this led to the standardization of stirrup-free SFRC beams in ACI 318,[38] such database does not yet exist for RAC beams reinforced with steel fibers and therefore additional research is necessary to build up a robust database. Moreover, limited guidelines are available for the design of RAC elements with steel fibers subjected to shear. Studies on stirrup-free beams with RAC cast with 100% RCA and steel fibers are also very limited.

This article studies experimentally and analytically the shear strength of stirrup-free RAC beams reinforced with steel fibers. Sixteen beams were tested in four-point bending using a shear-span-to-depth ratio (a/d) of 3.2. Fourteen of such beams were cast with RAC using 100% RCA reinforced internally with different fiber volume fractions (V_f = 0%, 0.5%, 0.75%, 1.0% or 1.5%), types of steel fibers (hook ends or double hook ends), and longitudinal reinforcement ratios (ρ_w= 1.6% and 2.5%). Another two control beams were cast with NAC without steel fibers. A new modification factor to the ACI 318-19 shear equation is also proposed to account explicitly for the effect of steel fibers and different longitudinal reinforcement ratios on the shear strength of RAC beams. The findings in this article contribute towards the development of practical guidelines for the design of RAC elements with steel fibers subjected to shear. The study also contributes with new experimental data of RAC beams reinforced with steel fibers, which builds up towards creating a robust database for standardization purposes. This, in turn, can lead to updates in building codes/standards that can promote the wider use of recycled materials in structural applications.

2. Materials and methods

The experimental program involved testing sixteen reinforced concrete beams without shear reinforcement. The investigated variables included the steel fiber volume fraction, fiber types, and longitudinal reinforcement. The materials, mix proportions and details of the beams are described in the following sections.

2.1 Material properties

The concrete mixes included Type 1 Ordinary Portland Cement (OPC), NCA, RCA, natural fine aggregate (FA), water, and superplasticizer (SP). The RCA was prepared by crushing waste concrete cylinders with a compressive strength of approximately 30 MPa (Fig. S1a). A low-cost machine (Fig. S1b) crushed the cylinders, which resulted in the RCA shown in Fig. S1c.

The NCA and RCA used in this study had a maximum size of approximately 19 mm, the typical maximum size used in concrete for structural elements in Thailand. The specific gravity and water absorption of the RCA were 2.4 and 4.59%, respectively, while the corresponding values of NCA were 2.7 and 0.28%. The properties of NCA, RCA, and natural fine aggregate (FA) are summarized in Table 1.

The diameter of the steel bars used as main longitudinal reinforcement was 16 mm and 20 mm. The nominal diameter of the shear reinforcement used in the control beams was 6 mm. The yield and ultimate stresses of the reinforcing steel are shown in Table 2. Commercial Dramix® steel fibers were used (Fig. 1). The mechanical properties of the two types of

Table 1. Physical properties of aggregates.

Properties	FA	NCA	RCA
Bulk Specific Gravity (SSD)	2.6	2.7	2.4
Unit Weight (kg/m^3)	-	1730	1397
Water Absorption (%)	0.54	0.28	4.59
Moisture (%)	0.1	0.61	2.24
Fineness Modulus	2.7	-	-
Max. size (mm)	4.76	19.1	18.6

fibers (3D and 4D) utilized in this study are shown in Table 3. These properties were provided by the manufacturer of the fibers.

Table 2. Mechanical properties of steel reinforcement.

Nominal size (mm)	Yield Stress (MPa)	Ultimate Stress (MPa)	Elongation (%)
20	540	656	17
16	549	640	22
6	402	590	29

2.2 Concrete mix proportions

Concrete mixes were designed and produced to attain a balance between workability and strength. The mixes had a water-cement ratio of 0.5 and a target compressive strength of 40 MPa. Two beams were cast for each mix design, one beam with 16 mm longitudinal bars (ρ_w = 1.6%), and one beam with 20 mm longitudinal bars (ρ_w = 2.5%), according to Table 4. Cement, water, and natural fine aggregate used in mix proportion were 500 kg, 250 kg, and 765 kg, respectively. Superplasticizer was also added to increase the workability of the mixes. Table 4 also lists the different volume fractions of 3D or 4D fibers used in the tests (V_f = 0%, 0.5%, 0.75%, 1.0% or 1.5%). The selected fiber volume fractions are typically adopted by contractors in the construction of SFRC floors and slabs-on-grade. The beam ID is also shown in Table 4, which begins with the beam number, followed by the fiber volume fraction and type of fiber. Bar sizes are at the end to distinguish different longitudinal reinforcements. For instance, F1-3D-DB20 corresponds to a beam with 1.0% of steel fibers (3D type) with 20-mm bars (DB20) used as longitudinal reinforcement (ρ_w = 2.5%).

Table 3. Mechanical properties of steel fibers.

Properties	3D Fibers (Hook Ends)	4D Fibers (Double Hook Ends)
Tensile Strength (MPa)	1125	1500
Length (mm)	60	60
Diameter (mm)	0.75	0.9
Aspect Ratio (l/d)	80	65

2.3 Beam geometry

The beams had a rectangular cross-section of 150 × 200 mm, and a total length of 1800 mm (see Fig. 2). The effective depth of the beams was maintained at 170 mm, with a shear-span-to-depth ratio (a/d) of 3.2. A constant concrete cover of 20 mm was adopted. The beams were designed to have two longitudinal reinforcement ratios in order to produce under-reinforced sections: eight beams with two 16 mm bars (ρ_w = 1.6%), and eight beams with two 20 mm bars (ρ_w = 2.5%). Accordingly, the beams are divided into two series: series DB16 for beams with 16 mm bars, and series DB20 for beams with 20 mm bars. Two 6 mm longitudinal bars were also added as top reinforcement (Fig. 2(b)). Stirrups, made from 6-mm round steel bars, were installed along 2/3 of the beam length at a 100 mm spacing (see Side A in Fig. 2(a)).

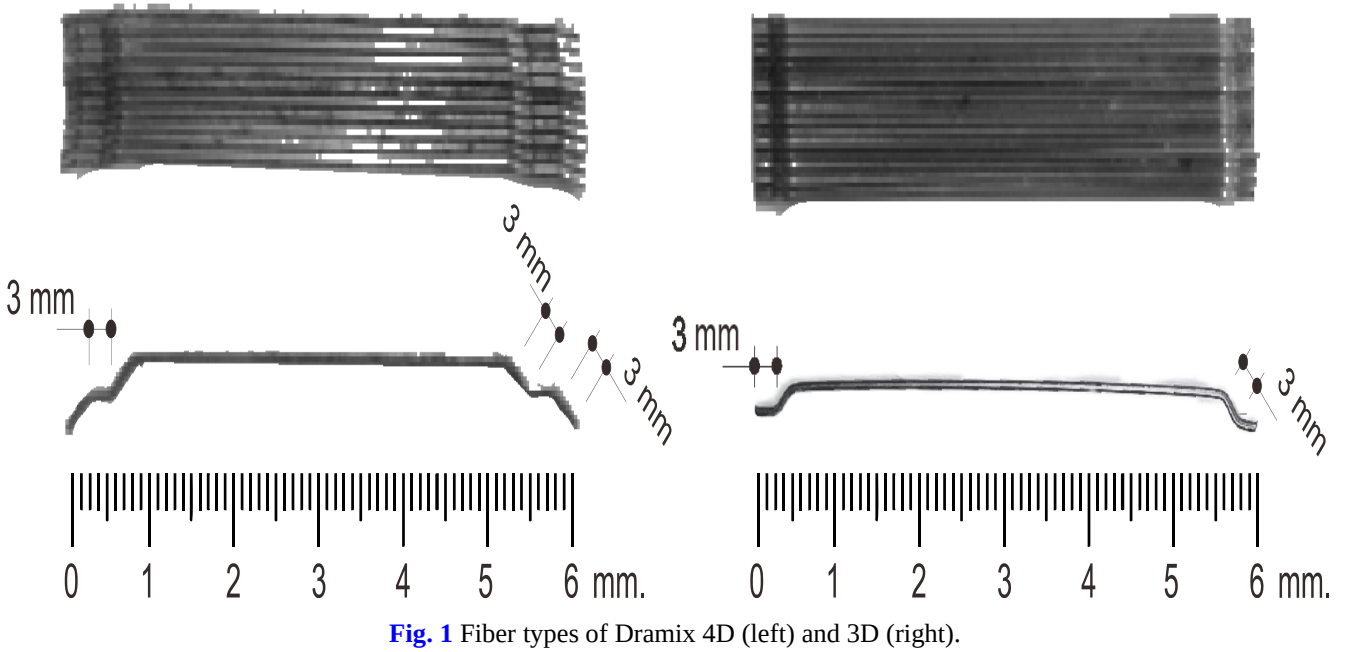

Fig. 1 Fiber types of Dramix 4D (left) and 3D (right).

Table 4. Concrete mix proportions and ID of beams.

No.	ID	Fiber (%)	ρ_w (%)	Concrete mix proportions (kg/m^3)			
				NCA	RCA	Fibers	Superplasticizer
B1	F0-DB16-N	0	1.6	768	-	-	1.25
B2	F0-DB16	0	1.6	-	768	-	1.25
B3	F0.5-3D-DB16	0.5	1.6	-	768	39.0	1.50
B4	F0.75-3D-DB16	0.75	1.6	-	768	58.5	1.50
B5	F1-3D-DB16	1.0	1.6	-	768	78.0	1.60
B6	F1.5-3D-DB16	1.5	1.6	-	768	117.0	1.60
B7	F0.75-4D-DB16	0.75	1.6	-	768	58.5	1.50
B8	F1-4D-DB16	1.0	1.6	-	768	78.0	1.60
B9	F0-DB20-N	0	2.5	768	-	-	1.25
B10	F0-DB20	0	2.5	-	768	-	1.25
B11	F0.5-3D-DB20	0.5	2.5	-	768	39.0	1.50
B12	F0.75-3D-DB20	0.75	2.5	-	768	58.5	1.50
B13	F1-3D-DB20	1.0	2.5	-	768	78.0	1.60
B14	F1.5-3D-DB20	1.5	2.5	-	768	117.0	1.60
B15	F0.75-4D-DB20	0.75	2.5	-	768	58.5	1.50
B16	F1-4D-DB20	1.0	2.5	-	768	78.0	1.60

The rest of the beam (Side B in Fig. 2(a)) was deliberately left without stirrups to assess the effectiveness of steel fibers as an alternative to conventional shear stirrups. This was also done to understand the role of steel fibers in preventing shear failures. All the beam reinforcement met the ACI 318-19[42] requirements, thus representing typical solutions adopted in practical designs. As a result, all beams were expected to fail primarily by shear at the unreinforced Side B. Fig. S2 shows a typical photo of a beam (F0-DB16-N) just before testing.

2.4 Test setup and testing procedure

The beams were subjected to four-point bending after 28 days of casting, according to the arrangement shown in Fig. 2(a). The beams were simply supported on roller and pin supports, with a 1600-mm clear span. Two linear variable differential transformers (LVDTs) were positioned at the mid-span of the beams (one of each beam's faces) to measure vertical deflections. Likewise, two vertical LVDTs were also placed at the beam's supports (Fig. 2(a)). The effective deflections at the mid-span of the beams were then calculated by subtracting the uplift recorded by the two LVDTs at both supports from the initial mid-span LVDT readings. A 1000 kN jack applied increasing load to a transfer beam resting on the top of the beams. The load was applied gradually until the beams failed.

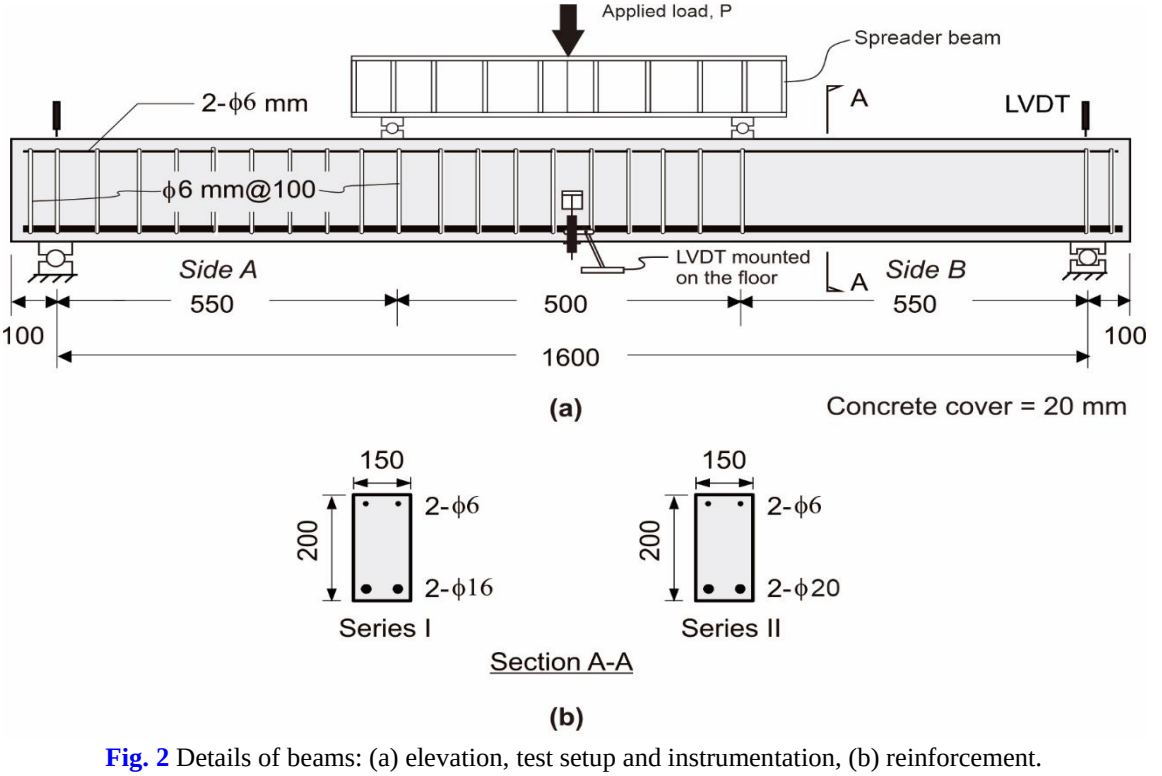

Fig. 2 Details of beams: (a) elevation, test setup and instrumentation, (b) reinforcement.

Load and deflections were monitored and recorded by a data acquisition system. On the same testing day, three concrete cylinders (diameter of 150 mm and height of 300 mm) were tested to determine the compressive strength of the concrete.

3. Results and discussion

A summary of test results is shown in Table 5, including average concrete compressive strength (f'_c), yielding load (P_y), ultimate load (P_u), calculated shear strength (V_{test}), normalized shear stress ($V_{test}/(bd\sqrt{f'_c})$), and failure modes. The main results are discussed in the following sections.

The data in Table 5 indicate that whilst pairs of beams were cast with the same mix concrete proportions, the compressive strength on the testing day was sometimes slightly different. Such differences in f'_c can be attributed to several factors, including the natural (and unavoidable) variability of concrete, the variable physical properties of RCA (which is often heterogeneous even within the same RCA batch), minor variations in mixing and vibration (the latter was done by hand using a portable poker), and the presence of steel fibers. Moreover, only one beam was tested per day, and therefore additional strength could have developed over the testing period (20+ days).

3.1 Ultimate load and failure behavior

As expected, the beams without steel fibers (B1, B2, B9, B10) failed in shear, as illustrated by the typical diagonal shear cracking observed during the tests (see Fig. S3 and S4). Beams with modest fiber volume fractions V_f of 0.5% and 0.75% (B3, B11, B12, B15) also experienced shear failure. The eight remaining RAC beams experienced a flexural failure instead, which can be attributed to the steel fibers acting as shear reinforcement. Table 5 presents the ultimate load and shear strength, equivalent to half of the ultimate loads. Although eight of the RAC beams experienced flexural failure, the shear strength for those beams was conservatively estimated to be half of the ultimate load in this study.

Including steel fibers at volume fractions of 0.75%, 1.0% or 1.5% in other beams in the DB16 series (ρ_w = 1.6%) changed the shear failure into a flexural failure, as depicted in Fig. S3. Moreover, the ultimate strengths of the beams increased with the amount of steel fibers, thus confirming the positive effect of steel fibers on the beams' overall strength. The results suggest that the steel fibers acted as the traditional shear reinforcement they intend to replace, increasing the shear strength of the beams above their flexural strength and thus forcing the beams to fail in flexure.

As for the shear failure of the beams in Fig. S3 and S4, it was observed that beams without steel fibers experienced a shear failure on the unreinforced Side B (i.e. without stirrups), with approximately 45° inclination angles. Small vertical cracks were also observed within the beams' mid-span, and these propagated towards the supports. On the other hand, beams with fibers exhibited multiple vertical cracks at the mid-span. These cracks then spread diagonally and led to combined flexural-shear cracks. The test results also indicate that the steel fibers helped reduce the crack widths, thus resisting more effectively the diagonal tension in the section and increasing the shear strength.

3.2 Load-deflection responses

Figure 3 compare, respectively, the load vs mid-span deflection curves for beams with reinforcement ratios ρ_w = 1.6% (series DB16) and ρ_w = 2.5% (series DB20). From the results in Table 5 and Fig. 3(a), it is evident that beams B1 (F0-DB16-N) and B2 (F0-DB16) only exhibited small cracks

Table 5. Summary of results of tested beams.

No.	ID	f'_c (MPa)	COV of f'_c (%)	P_y (kN)	P_u (kN)	V_{test} (kN)	Shear Stress $V_{test}/(bd\sqrt{f'_c})$	Failure Mode
B1	F0-DB16-N	34.2	3.9	-	67.0	33.5	0.22	Shear
B2	F0-DB16	41.1	4.2	-	73.7	36.85	0.22	Shear
B3	F0.5-3D-DB16	37.5	2.3	-	106.2	53.1	0.34	Shear
B4	F0.75-3D-DB16	40.8	3.2	116.3	120.2	60.1	0.36	Flexure
B5	F1-3D-DB16	41.3	3.8	114.7	119.6	59.8	0.36	Flexure
B6	F1.5-3D-DB16	44.7	4.2	119.7	149.8	74.9	0.43	Flexure
B7	F0.75-4D-DB16	44.6	4.1	117.1	130.9	65.45	0.38	Flexure
B8	F1-4D-DB16	45.7	3.5	118.2	125.2	62.6	0.36	Flexure
B9	F0-DB20-N	37.0	4.4	-	101.3	50.65	0.33	Shear
B10	F0-DB20	37.2	3.4	-	83.2	41.6	0.27	Shear
B11	F0.5-3D-DB20	37.5	4.3	-	129.2	64.6	0.41	Shear
B12	F0.75-3D-DB20	45.3	4.1	-	144.5	72.25	0.42	Shear
B13	F1-3D-DB20	45.4	3.1	162.3	165.7	82.85	0.48	Flexure
B14	F1.5-3D-DB20	37.7	3.2	182.9	185.4	92.7	0.59	Flexure
B15	F0.75-4D-DB20	44.1	2.6	161.2	163.2	81.6	0.48	Shear
B16	F1-4D-DB20	44.1	3.3	162.2	163.0	81.5	0.48	Flexure

and underwent less than 6 mm deflection at the mid-span before a sudden failure occurred at Side B. This type of failure is common for beams without shear reinforcement. The ultimate beam strengths were 67 kN for B1 (F0-DB16-N) and 73.7 kN for B2 (F0-DB16), respectively. Adding a V_f of 0.5% of 3D steel fibers in beam B3 (F0.5-3D-DB16) improved its shear strength, and its ultimate load increased to 106.2 kN. A small defection of 8 mm and tiny cracks were observed in this beam before a sudden shear failure occurred. With the increase in steel fibers V_f from 0.75% to 1.5% in B4 (F0.75-3D-DB16), B5 (F1-3D-DB16), and B6 (F1.5-3D-DB16), the ultimate loads were increased by 1.63, 1.62, and 2.03 times, respectively, compared to the counterpart RAC beam without steel fibers B2 (F0-DB16). Larger deflections above 25 mm were measured in these RAC beams. This confirms the effectiveness of steel fibers at increasing the tensile strength of RAC after post-cracking and at altering the failure mode from shear to flexure.

Figure 3(b) shows the response of beams in the DB20 series (ρ_w = 2.5%). Beams B9 (F0-DB20-N) and B10 (F0-DB20) showed similar behavior compared to B1 (F0-DB16-N) and B2 (F0-DB16). They underwent small deflections of less than 8 mm and tiny cracks before a shear failure occurred. Beam B11 (F0.5-3D-DB20), B12 (F0.75-3D-DB20), and B15 (F0.75-4D-DB20) also experienced a shear failure despite adding V_f of 0.5% and 0.75% of steel fibers. However, the steel fibers effectively increased the ultimate loads in these beams by more than 1.6 times compared to those without steel fibers. Multiple cracks were visible along the beam length with larger deflections than those without fibers. With V_f of 1.0% and 1.5% steel fibers, the shear failures were prevented in the beams, as shown in Fig. S3. The beams sustained multiple cracks and large deflections beyond 25 mm before concrete crushing occurred at the top of the beam. The steel fibers controlled the crack width in these beams, primarily by increasing the concrete tensile strength.

Figure 4 compare, respectively, the normalized shear stress vs mid-span deflection curves for beams with reinforcement ratios ρ_w = 1.6% and ρ_w = 2.5%. In these figures, the shear stresses (V_{test}/bd, where b =150 mm, and d = 170 mm) were normalized by the square root of compressive cylinder strength f'_c to fairly assess the results. The results indicate that, for beams with ρ_w = 1.6% (DB16 series), the normalized shear stresses between B1 and B2 were similar. However, the normalized shear stresses for B3, B4, B5 and B6 were higher by 1.5, 1.6, 1.7 and 1.9 times that of B2, respectively. Similar trends were observed for RAC beams with ρ_w = 2.5% (series DB20), where the normalized shear stresses of beams B11, B12, B13, and B14 increased respectively by 1.5, 1.6, 1.8, and 2.2 times over that of B10. However, the RAC beam without fibers in this series (B10) had a lower shear stress (by 18%) compared to that of the control NAC beam (B9). Adding steel fibers of 0.5% volume fraction to RAC beams significantly improved the normalized shear stresses by 51% and 55% for beams with ρ_w of 1.6% and 2.5%, respectively. It is noted that the shear stresses of all RAC beams with steel fibers effectively sustained shear stresses above $0.3\sqrt{f'_c}$ (shown as a dashed line in Fig. 4), which is the lowest bound shear stress recommended in ACI 318 for RC beams with steel fibers used as shear reinforcement.

3.3 Effect of fiber volume fraction

The normalized shear stresses ($V_{test}/bd\sqrt{f'_c}$) vs steel fiber volume fraction (V_f) are compared in Fig. 5 for the RAC beams reinforced with steel fibers. The results indicate an increase in shear strength as the fiber volume fraction increased, similar to SFRC beams with cast with NAC. For RAC beams with a ratio ρ_w = 1.6% (series DB16), the beams with 3D steel fibers at V_f of 0.5%, 0.75%, 1.0% and 1.5% had normalized shear stresses of 51%, 64%, 66%, and 95% higher than the RAC beams without the fibers. Likewise, for beams with a ratio ρ_w = 2.5% (series DB20), the normalized shear stress of RAC beams with V_f of 0.5% and 1.5% fibers was 54% and 121%, respectively, being thus higher than that of the RAC beams without 3D fibers. The difference between a V_f of

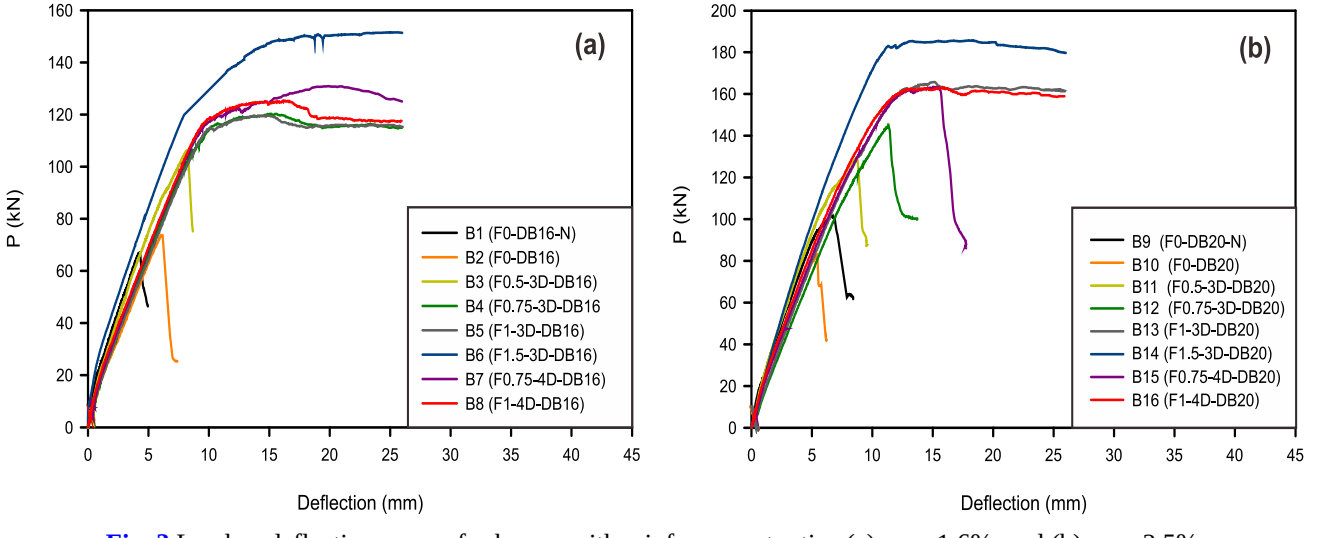

Fig. 3 Load vs deflection curves for beams with reinforcement ratios (a) ρ_w = 1.6%, and (b) ρ_w = 2.5%.

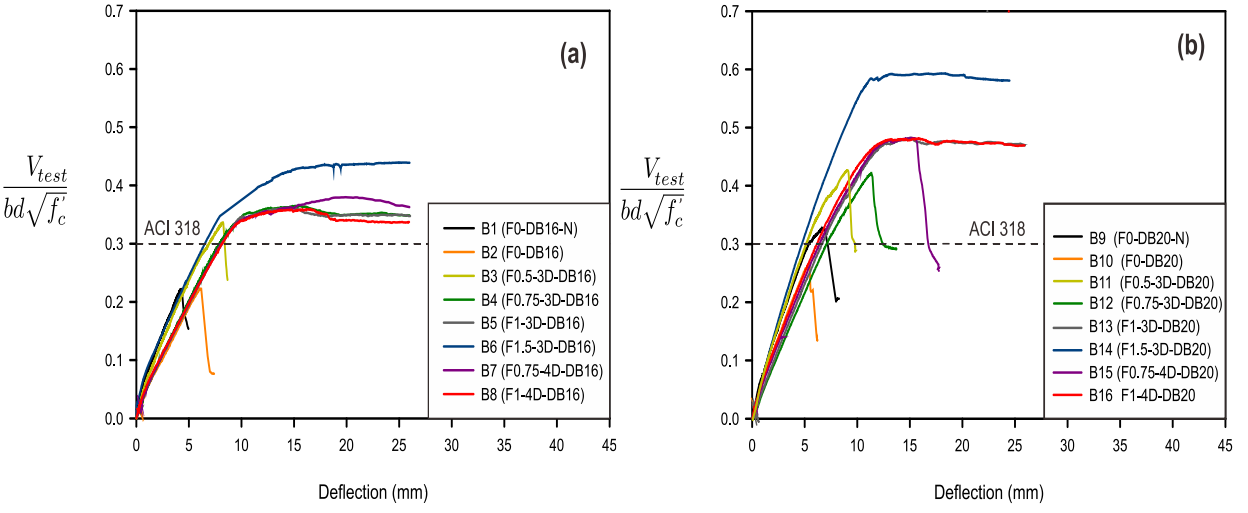

Fig. 4 Normalized shear stress vs. deflection for beams with longitudinal reinforcement ratios (a) ρ_w = 1.6%, and (b) ρ_w = 2.5%.

fibers 0.5% and 0.75% led to a slight increase in shear stresses for RAC beams in this series. In both series of RAC beams, the effectiveness of steel fibers in preventing shear failure at V_f of 0.5% and 0.75% is marginal.

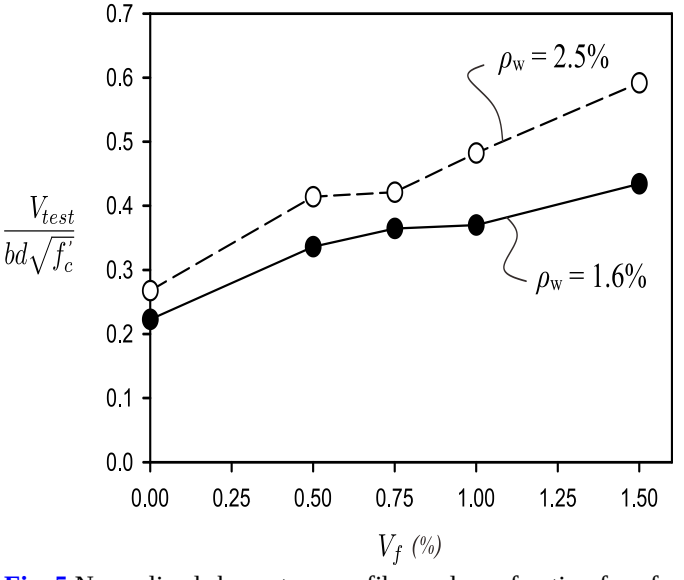

Fig. 5 Normalized shear stress vs fiber volume fraction for of RAC beams with reinforcement ratios ρ_w = 1.6% and 2.5%.

3.4 Effect of longitudinal reinforcement ratio

The effect of the longitudinal reinforcement ratios on the shear strength of fiber-reinforced RAC beams was evaluated using the two longitudinal reinforcement ratios adopted here, i.e. ρ_w = 1.6% and 2.5%. A previous study[20] showed that the longitudinal reinforcement contributes to the shear resistance of RAC beams without stirrups. Moreover, the shear equation in ACI 318-19 was modified to conservatively estimate the shear strength of RAC beams without stirrups.

Figure 5 compares RAC beams with steel fibers at different volume fraction *(V_f)* for two longitudinal reinforcement ratios. For RAC beams without steel fibers, the beam B10 in the series DB20 (with ρ_w = 2.5%) had 23% higher shear strength than the beam B2 in the DB16 series (with ρ_w = 1.6%). For steel fibers of 0.5% volume fraction, the beam B11 with ρ_w = 2.5% had 20.6% higher shear strength than the beam B3 (with ρ_w = 1.6%). For V_f above 0.75%, the effect of longitudinal reinforcement ratios on shear strength could not be accurately determined because the steel fibers prevented shear failure, and flexural failure modes occurred instead. However, an increase in shear stress of at least 17%, 30% and 37% for fibers at V_f of 0.75%, 1.0%, and 1.5% was conservatively estimated for RAC beams with ρ_w = 2.5% compared to counterpart beams with ρ_w = 1.6%. These results confirm that the amount of longitudinal reinforcement can contribute to the shear resistance of RAC beams.

3.5 Effect of fiber type

The normalized shear stresses of RAC beams with 3D and 4D steel fibers is shown in Fig. 6. For beams with ρ_w = 1.6% (series DB16 in Fig. 6(a)), the responses of four of the RAC beams (B4 vs B7 and B5 vs B8) were similar. Their stiffness, failure modes, and ultimate loads were virtually identical. Both types of steel fibers (3D and 4D) improved the beams' shear strength effectively, so that their shear strengths were higher than their flexural strength and changed the failure modes from shear to flexure.

The impact of 4D steel fibers was more evident for RAC beams with a higher longitudinal reinforcement ratio of ρ_w = 2.5% (series DB20). For beams with ρ_w = 2.5% and steel fibers at V_f of 0.75%, B15 with 4D fibers showed higher shear strength than B12 with 3D fibers by 14%, as depicted in Fig. 6(b). This higher ultimate strength was attributed to the higher tensile strength of 4D steel fibers. However, the effect of 4D fibers was not observed for steel fibers at 1.0% (B13 vs B16) since including 1.0% steel fibers of both types altered the shear failure to flexural failure in both beams.

3.6 Bending moment capacities

The experimental and calculated yielding and ultimate

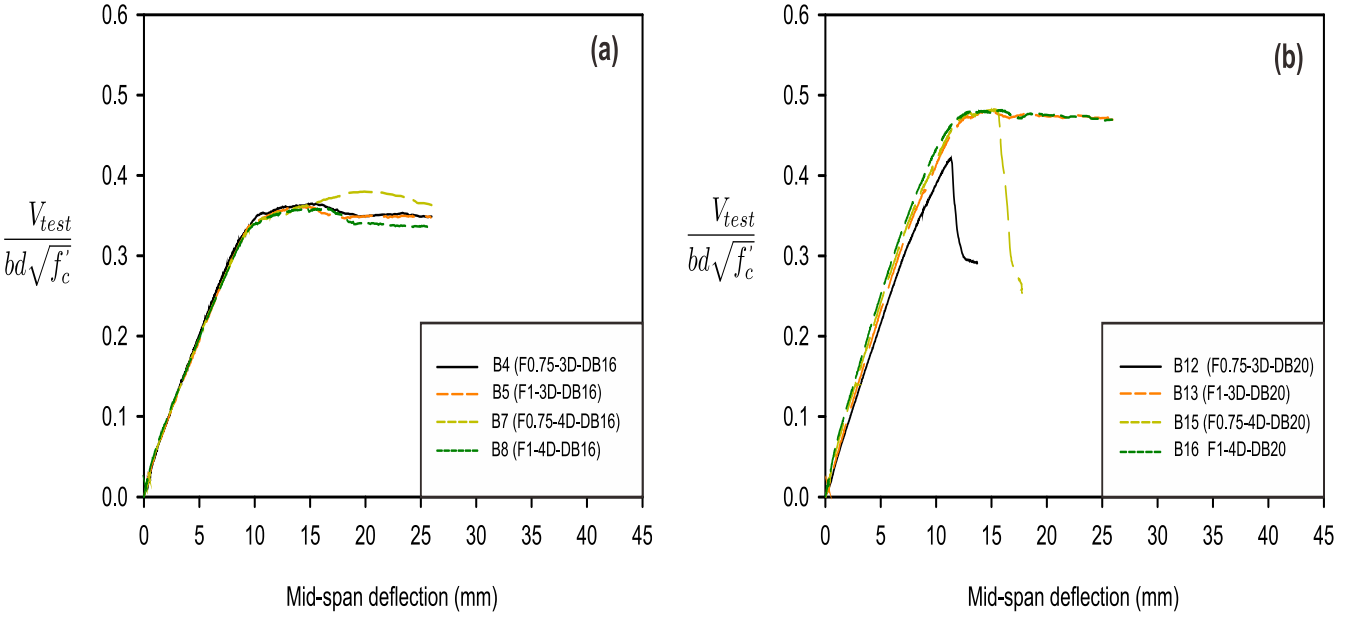

Fig. 6 The normalized shear stresses with different fiber types for beams with reinforcement ratio (a) ρ_w = 1.6%, and (b) ρ_w = 2.5%.

moment capacities of the tested beams are summarized in Table 6. The calculated moment capacities are based on ACI 318 by neglecting the strain hardening of steel reinforcement and the tensile resistance from the steel fibers. The results show that the steel fibers can enable ductile flexural failures in eight beams with V_f of 0.75% and 1.0% for longitudinal reinforcement ratios ρ_w = 1.6% and 2.5%, respectively. Conversely, the other eight beams failed by shear because their shear strengths were lower than moment capacities. The results also show that the use of a V_f of 0.5% was insufficient to enhance the shear strength of beams without stirrups (see B3 and B11). This is consistent with the ACI 318 recommendations that allows the total replacement of shear reinforcement with steel fibers but with at least a V_f of 0.75%. Therefore, the ultimate moments for these beams (B1-B4, and B9-B12) are much lower than calculated ultimate moments. This behavior is corroborated by the low toughness experienced by such beams, with energy absorptions <1000 kNmm for most beams.

Table 6 also shows that, for beams B4-B8, B13-B14, and B16, the ductile behavior is enhanced by adding steel fibers at V_f of 0.75%, 1.0%, and 1.5%. These beams mobilized their full flexural capacities even without shear reinforcement since the steel fibers improved their post-cracking behavior in shear. The yielding observed in the tests (see yielding plateaus in Fig. 3) and ultimate moments for these beams agree well with the predicted moment capacities, as shown in Table 6. The toughness of RAC beams also significantly improved by 8.7

Table 6. Summary of yielding and ultimate moments of tested beams.

No.	ID	$M_{y,test}$ (kNm)	$M_{y,cal}$ (kNm)	$M_{u,test}$ (kNm)	$M_{u,cal}$ (kNm)	$M_{u,test}$ / $M_{u,cal}$	Toughness (kNmm)
B1	F0-DB16-N	-	-	18.4	31.6	-	202
B2	F0-DB16	-	-	20.2	32.6	-	290
B3	F0.5-3D-DB16	-	-	29.2	32.1	-	543
B4	F0.75-3D-DB16	32.0	31.8	33.1	32.5	1.02	2510
B5	F1-3D-DB16	31.5	31.9	32.9	32.6	1.01	2487
B6	F1.5-3D-DB16	32.9	32.0	41.2	33.0	1.25	3154
B7	F0.75-4D-DB16	32.2	32.0	36.0	32.9	1.09	2681
B8	F1-4D-DB16	32.5	32.0	34.4	33.0	1.04	2597
B9	F0-DB20-N	-	-	27.9	44.9	-	545
B10	F0-DB20	-	-	22.9	44.9	-	296
B11	F0.5-3D-DB20	-	-	35.5	45.0	-	761
B12	F0.75-3D-DB20	-	-	39.7	47.2	-	1166
B13	F1-3D-DB20	44.6	46.7	45.6	47.2	0.97	3342
B14	F1.5-3D-DB20	50.3	45.6	51.0	45.1	1.13	3874
B15	F0.75-4D-DB20	-	-	44.8	46.9	-	1921
B16	F1-4D-DB20	44.6	46.2	44.8	46.9	0.96	3361

times by adding 0.75% steel fibers into the beam with ρ_w = 1.6%conservatively adopted for RAC beams with the 3D and 4D (B4) compared to the RAC beam without steel fibers (B2). steel fibers used in this study.

4. Prediction of concrete shear strength

4.1. Ultimate concrete shear strength

ACI 318-19 provides two shear equations for concrete beams, which can be used for beams with at least the minimum shear reinforcement:

$$V_c = 0.17\lambda\sqrt{f_c'}bd \quad (1)$$

$$V_c = 0.66\lambda(\rho_w)^{1/3}\sqrt{f_c'}bd \quad (2)$$

where λ is a reduction factor for lightweight aggregate, f'_c is the concrete compressive strength (in MPa), b is the beam width (in mm), d is the effective depth (in mm), and ρ_w is the longitudinal reinforcement ratio.

For beams with stirrups below those required for shear reinforcement, the shear equations are:

$$V_c = 0.66\lambda_s\lambda(\rho_w)^{1/3}\sqrt{f_c'}bd \quad (3)$$

where λ_s is the size effect modification factor, that can be calculated as:

$$\lambda_s = \sqrt{\frac{2}{1+0.004d}} \leq 1 \quad (4)$$

Table 5 and Fig. 4 compare the normalized shear stresses for RAC beams with steel fibers and the ACI 318-19 provisions. Parra-Montesinos et al.[53,54] suggested that reinforced concrete beams with deformed steel fibers with at least a V_f of 0.75% exhibited failure shear stresses above $0.3\sqrt{f_c'}$. Accordingly, this conservative lower bound was adopted in ACI 318-19 for reinforced concrete beams built with steel fibers as shear reinforcement. In this study, the tested RAC beams with steel fibers with V_f of 0.5% to 1.5% exhibited shear stresses above the conservative lower bound value of $0.3\sqrt{f_c'}$, as indicated by the dashed lines in Fig. 4. This suggests that the ACI 318-19 provisions for shear of beams built with SFRC can also be

4.2 A New equation for shear prediction of RAC beams with steel fibers

Table 7 summarizes the shear stress ratios of all beams tested in this study. Equation (3) was used to calculate V_c, as shown in column (4) of Table 7. Fig. 7 shows the relationship between shear strength ratios (V_{test}/V_c) and steel fiber volume fractions (V_f). It is clear that the addition of more fibers helped improve the shear strength of the beams. A linear relationship was also determined, as shown by the dotted line in Fig. 7.

A new practical modification factor k obtained from the linear relationship shown in Fig. 7 was incorporated into Equation 3, thus leading to the proposed Equation (5):

$$V_{proposed} = 0.66\lambda_s k(\rho_w)^{1/3}\sqrt{f_c'}bd \quad (5)$$

$$\text{where: } k = 0.92V_f + 1.51, \text{ for } 0.5\% \leq V_f \leq 1.5\% \quad (6)$$

Equation 5 was then used to calculate the shear strength of the beams ($V_{proposed}$), as listed in column 6 of Table 7. It is shown that the shear predictions from the proposed equation were relatively close to the experimental results, as shown by $V_{test}/V_{proposed}$ ratios close to one (see last column of Table 7).

5. Practical implications

The enhanced shear strength and improved post-cracking behavior of steel fiber-reinforced RAC make it a promising material for use in different structural elements. In beams in particular, the ability of steel fibers to bridge cracks can help recover the strength of RAC and change its traditionally brittle behavior into a more ductile one, thus increasing the resilience of RAC structures. Steel fiber-reinforced RAC can also be used in other structural members subjected to high shear stresses, such as flat slabs,[55] corbels[56] and short/squat

Table 7. Summary of shear strength ratios.

No.	ID	V_f (%)	V_{test} (kN)	V_c (kN)	V_{test} / V_c	$V_{proposed}$ (kN)	V_{test} / $V_{proposed}$
(1)		(2)	(3)	(4)	(5)	(6)	(7)
B1	F0-DB16-N	0	33.5	24.9	1.3	-	-
B2	F0-DB16	0	36.9	27.3	1.4	-	-
B3	F0.5-3D-DB16	0.5	53.1	26.0	2.0	51.4	1.03
B4	F0.75-3D-DB16	0.75	60.1	27.2	2.2	59.9	1.01
B5	F1-3D-DB16	1.0	59.8	26.7	2.2	65.1	0.92
B6	F1.5-3D-DB16	1.5	74.9	28.4	2.6	82.3	0.91
B7	F0.75-4D-DB16	0.75	65.5	28.4	2.3	62.6	1.05
B8	F1-4D-DB16	1.0	62.6	28.8	2.2	70.0	0.90
B9	F0-DB20-N	0	50.7	29.8	1.7	-	-
B10	F0-DB20	0	41.6	29.9	1.4	-	-
B11	F0.5-3D-DB20	0.50	64.6	30.0	2.2	59.2	1.09
B12	F0.75-3D-DB20	0.75	72.3	33.0	2.2	72.6	1.00
B13	F1-3D-DB20	1.0	82.9	33.0	2.5	80.3	1.03
B14	F1.5-3D-DB20	1.5	92.7	30.1	3.1	87.1	1.07
B15	F0.75-4D-DB20	0.75	81.6	32.5	2.5	71.7	1.14
B16	F1-4D-DB20	1.0	81.5	32.5	2.5	79.2	1.03

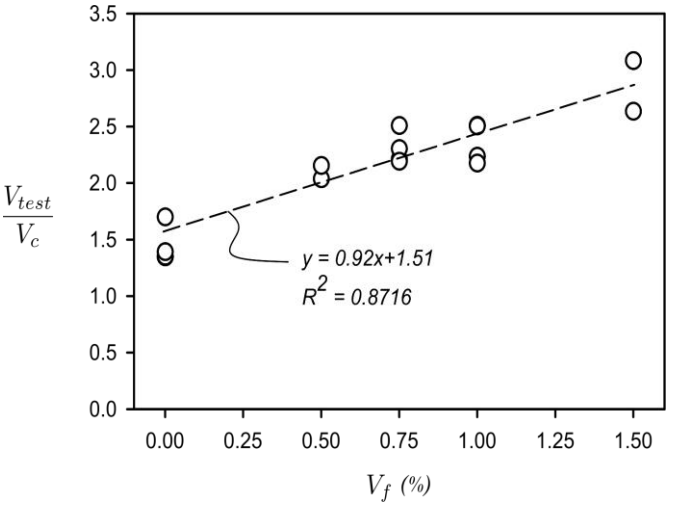

Fig. 7 Relationship between shear strength ratio and fiber volume fraction for tested beams.

columns.[57] Steel fiber-reinforced RAC can also be used for the rehabilitation of existing structures that are prone to shear deficiencies[51] or repair overlays,[58] offering a sustainable alternative to conventional strengthening techniques.

Moreover, the successful application of steel fiber-reinforced RAC in real-world projects could drive broader adoption of recycled materials in structural applications, reducing the reliance on natural aggregates and promoting the adoption of circular economy principles in the construction sector. This is relevant for Southeast Asia, a region which is lagging in this respect.

From a cost optimization perspective, the use of steel fibers can potentially replace traditional shear reinforcement like stirrups, thereby simplifying the construction process and reducing labor costs. Additionally, the improved mechanical properties of steel fiber-reinforced RAC can extend the service life of structures, leading to lower maintenance and repair costs over time. Moreover, by incorporating RCA, the demand for virgin materials and CDW are both reduced, thereby reducing the carbon footprint associated with aggregate extraction and transport. Additionally, the reduced need for traditional reinforcement, thanks to the use of steel fibers, can further cut down the carbon emissions associated with steel production and shipping. This shift towards low-carbon construction materials is necessary so that the construction sector can meet its climate targets. In this regard, the recycling and construction industries need to implement advanced methods for rapid CDW and RCA screening[59,60] so that the high demand for recycled materials can be met.

The results in this study also suggest that current code approaches to calculate/limit shear stresses in elements can be modified for the use of steel fiber-reinforced RAC. However, since this study conducted tests on a limited number of beams, the modification factor (Equation 6) proposed here may not fully capture the variability of other RAC reinforced with other types of steel fibers. Additional tests on RAC beams with steel fibers are recommended to validate the findings presented here and to corroborate if such modification factor is applicable to beams with other types of RAC (with different RCA replacement volumes) and different types of steel fibers. Likewise, beams with different cross sections, lengths and load arrangements should be tested to investigate any size effects and, if necessary, propose different modifications to the ACI 318 equation. It should be noted that whilst the focus of this study was on isolated beam elements, future research should also investigate the residual shear resistance of RAC beams with steel fibers using larger elements (*e.g.* a shear-deficient steel fiber-reinforced RAC frame).

6. Conclusions

This study conducted experimental and analytical investigations on the effect of steel fibers on the shear strength of recycled aggregate concrete (RAC) beams without stirrups. Natural coarse aggregates were totally substituted with recycled concrete aggregates (RCA) reinforced with steel fibers (hook ends or double hook ends) at different fiber volume fractions (V_f = 0%, 0.5%, 0.75%, 1.0% or 1.5%). Two longitudinal reinforcement ratios (ρ_w = 1.6% or 2.5%) were examined. A new modification factor to the ACI 318-19 shear equation is also proposed. Based on the experimental results, the following conclusions can be drawn.

- Compared to control RAC beams without steel fibers, the steel fibers with hook ends at V_f = 0.5% effectively improved the shear stresses of RAC beams by 51% and 55% at ρ_w = 1.6% and 2.5%, respectively.
- Adding steel fibers with hook ends at V_f = 0.75% prevented the shear failure of RAC beams with ρ_w = 1.6%. Moreover, for RAC beams with ρ_w = 2.5%, the steel fibers with hook ends at V_f = 1.0% prevented shear failures and changed them to flexural failures.
- The amount of longitudinal reinforcement impacted the shear strength of RAC beams with and without fibers. Increasing the longitudinal reinforcement ratios from 1.6% to 2.5% enhanced the shear capacity of RAC beams by 20.6% for steel fibers with hook ends at V_f = 0.5%.
- The effectiveness of steel fibers with double hook ends was more evident for RAC beams with high longitudinal reinforcement ratios ρ_w = 2.5%. For RAC beams with ρ_w = 1.6%, the impact of steel fibers with hook ends (3D) and double hook ends (4D) was similar.
- Steel fibers at V_f = 0.75% or higher can be effectively used instead of stirrups for RAC beams with ρ_w = 1.6% and above. Moreover, RAC beams with steel fibers of at least V_f = 0.75% can sustain shear stresses above $0.3\sqrt{f_c'}$. This value agrees with the conservative lower bound value included in ACI 318-19 for normal aggregate concrete beams with steel fibers replacing conventional stirrups.
- The use of the new modification factor into the ACI 318-19 equation led to good predictions of the shear stresses of the tested RAC beams reinforced with steel fibers. The factor explicitly accounts for the effect of the steel fibers and

different longitudinal reinforcement ratios. However, further research is needed to verify the accuracy of such equations at predicting the shear stress of other beams.

Acknowledgements
This research was supported by Thailand Science Research and Innovation Fund Contract No. FRB660041/0227.

Conflict of Interest
The authors declare that they do not have conflicts of interest.

Supporting Information
Not applicable.

References
[1] R. P. Neupane, T. Imjai, N. Makul, R. Garcia, B. Kim, S. Chaudhary, Use of recycled aggregate concrete in structural members: a review focused on Southeast Asia, *Journal of Asian Architecture and Building Engineering*, 2023, 1-24, doi: 10.1080/13467581.2023.2270029.
[2] R. V. Silva, J. De Brito, R. K. Dhir, Properties and composition of recycled aggregates from construction and demolition waste suitable for concrete production, *Construction and Building Materials*, 2014, **65**, 201-217, doi: 10.1016/j.conbuildmat.2014.04.117.
[3] S. C. Kou, C. S. Poon, Effect of the quality of parent concrete on the properties of high performance recycled aggregate concrete, *Construction and Building Materials*, 2015, **77**, 501-508, doi: 10.1016/j.conbuildmat.2014.12.035.
[4] J. De Brito, J. Ferreira, J. Pacheco, D. Soares, M. Guerreiro, Structural, material, mechanical and durability properties and behaviour of recycled aggregates concrete, *Journal of Building Engineering*, 2016, **6**, 1-16, doi: 10.1016/j.jobe.2016.02.003.
[5] N. Kisku, H. Joshi, M. Ansari, S. K. Panda, S. Nayak, S. C. Dutta, A critical review and assessment for usage of recycled aggregate as sustainable construction material, *Construction and Building Materials*, 2017, **131**, 721-740, doi: 10.1016/j.conbuildmat.2016.11.029.
[6] M. Etxeberria, E. Vázquez, A. Marí, M. Barra, Influence of amount of recycled coarse aggregates and production process on properties of recycled aggregate concrete, *Cement and Concrete Research*, 2007, **37**, 735-742, doi: 10.1016/j.cemconres.2007.02.002.
[7] F. Kefyalew, T. Imjai, R. Garcia, N. Khanh Son, S. Chaudhary, Performance of recycled aggregate concrete composite metal decks under elevated temperatures: a comprehensive review, *Journal of Asian Architecture and Building Engineering*, 2024, 1-23, doi: 10.1080/13467581.2024.2309347.
[8] A. Katz, Treatments for the improvement of recycled aggregate, *Journal of Materials in Civil Engineering*, 2004, **16**, 597-603, doi: 10.1061/(asce)0899-1561(2004)16: 6(597).
[9] V. W. Y. Tam, C. M. Tam, K. N. Le, Removal of cement mortar remains from recycled aggregate using pre-soaking approaches, *Resources, Conservation and Recycling*, 2007, **50**, 82-101, doi: 10.1016/j.resconrec.2006.05.012.
[10] S. C. Kou, C. S. Poon, Properties of concrete prepared with PVA-impregnated recycled concrete aggregates, *Cement and Concrete Composites*, 2010, **32**, 649-654, doi: 10.1016/j.cemconcomp.2010.05.003.
[11] K. K. Sagoe-Crentsil, T. Brown, A. H. Taylor, Performance of concrete made with commercially produced coarse recycled concrete aggregate, *Cement and Concrete Research*, 2001, **31**, 707-712, doi: 10.1016/s0008-8846(00)00476-2.
[12] K. N. Rahal, K. Elsayed, Shear strength of 50 MPa longitudinally reinforced concrete beams made with coarse aggregates from low strength recycled waste concrete, *Construction and Building Materials*, 2021, **286**, 122835, doi: 10.1016/j.conbuildmat.2021.122835.
[13] E. E. Etman, H. M. Afefy, A. T. Baraghith, S. A. Khedr, Improving the shear performance of reinforced concrete beams made of recycled coarse aggregate, *Construction and Building Materials*, 2018, **185**, 310-324, doi: 10.1016/j.conbuildmat.2018.07.065.
[14] M. Arezoumandi, A. Smith, J. S. Volz, K. H. Khayat, An experimental study on shear strength of reinforced concrete beams with 100% recycled concrete aggregate, *Construction and Building Materials*, 2014, **53**, 612-620, doi: 10.1016/j.conbuildmat.2013.12.019.
[15] A. M. Knaack, Y. C. Kurama, Behavior of reinforced concrete beams with recycled concrete coarse aggregates, *Journal of Structural Engineering*, 2015, **141**, B4014009, doi: 10.1061/(asce)st.1943-541x.0001118.
[16] M. Arezoumandi, J. Drury, J. S. Volz, K. H. Khayat, Effect of recycled concrete aggregate replacement level on shear strength of reinforced concrete beams, *ACI Materials Journal*, 2015, **112**, 559, doi: 10.14359/51687766.
[17] I. S. Ignjatović, S. B. Marinković, N. Tošić, Shear behaviour of recycled aggregate concrete beams with and without shear reinforcement, *Engineering Structures*, 2017, **141**, 386-401, doi: 10.1016/j.engstruct.2017.03.026.
[18] B. González-Fonteboa, F. Martínez-Abella, Shear strength of recycled concrete beams, *Construction and Building Materials*, 2007, **21**, 887-893, doi: 10.1016/j.conbuildmat.2005.12.018.
[19] S. Pradhan, S. Kumar, S. V. Barai, Shear performance of recycled aggregate concrete beams: an insight for design aspects, *Construction and Building Materials*, 2018, **178**, 593-611, doi: 10.1016/j.conbuildmat.2018.05.022.
[20] M. Setkit, S. Leelatanon, T. Imjai, R. Garcia, S. Limkatanyu, Prediction of shear strength of reinforced recycled aggregate concrete beams without stirrups, *Buildings*, 2021, **11**, 402, doi: 10.3390/buildings11090402.
[21] Han, B., H. Yun, and S. Chung, Shear capacity of reinforced concrete beams made with recycled-aggregate, *Special Publication*, 2001, **200**, 503-516, doi: 10.14359/10598.
[22] S. W. Kim, C. Y. Jeong, J. S. Lee, K. H. Kim, Size effect

in shear failure of reinforced concrete beams with recycled aggregate, *Journal of Asian Architecture and Building Engineering*, 2013, **12**, 323-330, doi: 10.3130/jaabe.12.323.
[23] H. B. Choi, C. K. Yi, H. H. Cho, K. I. Kang, Experimental study on the shear strength of recycled aggregate concrete beams, *Magazine of Concrete Research*, 2010, **62**, 103-114, doi: 10.1680/macr.2008.62.2.103.
[24] R. Sato, I. Maruyama, T. Sogabe, M. Sogo, Flexural behavior of reinforced recycled concrete beams, *Journal of Advanced Concrete Technology*, 2007, **5**, 43-61, doi: 10.3151/jact.5.43.
[25] M. Sogo, T. Sogabe, I. Maruyama, R. Sato, K. Kawai, Shear behavior of reinforced recycled concrete beams, Proceedings of the International RILEM Conference on the Use of Recycled Materials in Buildings and Structures, 2004.
[26] B. González-Fonteboa, F. Martínez-Abella, I. Martínez-Lage, J. Eiras-López, Structural shear behaviour of recycled concrete with silica fume, *Construction and Building Materials*, 2009, **23**, 3406-3410, doi: 10.1016/j.conbuildmat.2009.06.035.
[27] M. Etxeberria, A. R. Marí, E. Vázquez, Recycled aggregate concrete as structural material, *Materials and Structures*, 2007, **40**, 529-541, doi: 10.1617/s11527-006-9161-5.
[28] H. Katkhuda, N. Shatarat, Shear behavior of reinforced concrete beams using treated recycled concrete aggregate, *Construction and Building Materials*, 2016, **125**, 63-71, doi: 10.1016/j.conbuildmat.2016.08.034.
[29] H. D. Yun, W. C. Choi, Shear strength of reinforced recycled aggregate concrete beams without shear reinforcements, *Journal of Civil Engineering and Management*, 2017, **23**, 76-84, doi: 10.3846/13923730.2014.976257.
[30] S. Sadati, M. Arezoumandi, K. H. Khayat, J. S. Volz, Shear performance of reinforced concrete beams incorporating recycled concrete aggregate and high-volume fly ash, *Journal of Cleaner Production*, 2016, **115**, 284-293, doi: 10.1016/j.jclepro.2015.12.017.
[31] G. Wardeh, E. Ghorbel, Shear strength of reinforced concrete beams with recycled aggregates, *Advances in Structural Engineering*, 2019, **22**, 1938-1951, doi: 10.1177/1369433219829815.
[32] G. Fathifazl, A. G. Razaqpur, O. B. Isgor, A. Abbas, B. Fournier, S. Foo, Shear capacity evaluation of steel reinforced recycled concrete (RRC) beams, *Engineering Structures*, 2011, **33**, 1025-1033, doi: 10.1016/j.engstruct.2010.12.025.
[33] S. Leelatanon, T. Imjai, M. Setkit, R. Garcia, B. Kim, Punching shear capacity of recycled aggregate concrete slabs, *Buildings*, 2022, **12**, 1584, doi: 10.3390/buildings12101584.
[34] T. Imjai, P. Aosai, R. Garcia, S. N. Raman, S. Chaudhary, Deflections of high-content recycled aggregate concrete beams reinforced with GFRP bars and steel fibres, *Engineering Structures*, 2024, **312**, 118247, doi: 10.1016/j.engstruct.2024.118247.
[35] F. Kefyalew, T. Imjai, R. Garcia, B. Kim, Structural and service performance of composite slabs with high recycled aggregate concrete contents, *Engineered Science*, 2023, **27**, 1021, doi: 10.30919/es1021.
[36] T. Imjai, F. Kefyalew, P. Aosai, R. Garcia, B. Kim, H. M. Abdalla, S. N. Raman, A new equation to predict the shear strength of recycled aggregate concrete Z push-off specimens, *Cement and Concrete Research*, 2023, **169**, 107181, doi: 10.1016/j.cemconres.2023.107181.
[37] T. Imjai, R. Garcia, B. Kim, C. Hansapinyo, P. Sukontasukkul, Serviceability behaviour of FRP-reinforced slatted slabs made of high-content recycled aggregate concrete, *Structures*, 2023, **51**, 1071-1082, doi: 10.1016/j.istruc.2023.03.075.
[38] ACI 318-19 Building Code Requirements for Structural Concrete and Commentary, American Concrete Institute, 2019.
[39] D. Gao, W. Zhu, D. Fang, J. Tang, H. Zhu, Shear behavior analysis and capacity prediction for the steel fiber reinforced concrete beam with recycled fine aggregate and recycled coarse aggregate, *Structures*, 2022, **37**, 44-55, doi: 10.1016/j.istruc.2021.12.075.
[40] E. E. Anike, M. Saidani, A. O. Olubanwo, U. C. Anya, Flexural performance of reinforced concrete beams with recycled aggregates and steel fibres, *Structures*, 2022, **39**, 1264-1278, doi: 10.1016/j.istruc.2022.03.089.
[41] N. Kachouh, T. El-Maaddawy, H. El-Hassan, B. El-Ariss, Shear behavior of steel-fiber-reinforced recycled aggregate concrete deep beams, *Buildings*, 2021, **11**, 423, doi: 10.3390/buildings11090423.
[42] Y. E. Ibrahim, K. Fawzy, M. A. Farouk, Effect of steel fiber on the shear behavior of reinforced recycled aggregate concrete beams, *Structural Concrete*, 2021, **22**, 1861-1872, doi: 10.1002/suco.202000494.
[43] Y. Tan, C. Zhou, J. Zhou, Influence of the steel fiber content on the flexural fatigue behavior of recycled aggregate concrete, *Advances in Civil Engineering*, 2020, 8839271, doi: 10.1155/2020/8839271.
[44] N. Kachouh, H. El-Hassan, T. El-Maaddawy, Mechanical properties of recycled coarse aggregate concrete reinforced with steel fibers, *Proceedings of International Structural Engineering and Construction*, 2021, **8**, MAT-12-1-MAT-12-6, doi: 10.14455/ISEC.2021.8(1).
[45] M. Ghoneim, A. Yehia, S. Yehia, W. Abuzaid, Shear strength of fiber reinforced recycled aggregate concrete, *Materials*, 2020, **13**, 4183, doi: 10.3390/ma13184183.
[46] K. J. N. S. Nitesh, S. V. Rao, P. R. Kumar, An experimental investigation on torsional behaviour of recycled aggregate based steel fiber reinforced self-compacting concrete, *Journal of Building Engineering*, 2019, **22**, 242-251, doi: 10.1016/j.jobe.2018.12.011.
[47] M. C. Naoum, N. A. Papadopoulos, M. E. Voutetaki, C. E. Chalioris, Structural health monitoring of fiber-reinforced concrete prisms with polyolefin macro-fibers using a piezoelectric materials network under various load-induced stress, *Buildings*, 2023, **13**, 2465, doi: 10.3390/buildings13102465.

[48] N. A. Papadopoulos, M. C. Naoum, G. M. Sapidis, C. E. Chalioris, Cracking and fiber debonding identification of concrete deep beams reinforced with C-FRP ropes against shear using a real-time monitoring system, *Polymers*, 2023, **15**, 473, doi: 10.3390/polym15030473.
[49] A. Nzambi, D. Oliveira, Steel fiber reinforced concrete beams with predetermined failure surface and no stirrups, *Engineering Structures*, 2023, **290**, 116339, doi: 10.1016/j.engstruct.2023.116339.
[50] N. Kachouh, T. El-Maaddawy, H. El-Hassan, B. El-Ariss, Shear response of recycled aggregates concrete deep beams containing steel fibers and web openings, *Sustainability*, 2022, **14**, 945, doi: 10.3390/su14020945.
[51] H. Shabani Attar, M. Reza Esfahani, A. Ramezani, Experimental investigation of flexural and shear strengthening of RC beams using fiber-reinforced self-consolidating concrete jackets, *Structures*, 2020, **27**, 46-53, doi: 10.1016/j.istruc.2020.05.032.
[52] C. E. Chalioris, Analytical approach for the evaluation of minimum fibre factor required for steel fibrous concrete beams under combined shear and flexure, *Construction and Building Materials*, 2013, **43**, 317-336, doi: 10.1016/j.conbuildmat.2013.02.039.
[53] G. J. Parra-Montesinos, Shear strength of beams with deformed steel fibers, *ACI Concrete International*, 2006, **28**, 57-66.
[54] H. H. Dinh, G. J. Parra-Montesinos, J. K. Wight, Shear behavior of steel fiber-reinforced concrete beams without stirrup reinforcement, *ACI Structural Journal*, 2010, **107**, 597-606, doi: 10.14359/51663913.
[55] A. Blanco, P. Pujadas, A. De la Fuente, S. H. P. Cavalaro, A. Aguado, Influence of the type of fiber on the structural response and design of FRC slabs, *Journal of Structural Engineering*, 2016, **142**, 04016054, doi: 10.1061/(asce)st.1943-541x.0001515.
[56] T. S. Mustafa, F. B. A. Beshara, A. A. Mahmoud, M. M. A. Khalil, An improved strut-and-tie model to predict the ultimate strength of steel fiber-reinforced concrete corbels, *Materials and Structures*, 2019, **52**, 1-9, doi: 10.1617/s11527-019-1363-8.
[57] A. Venkateshwaran, B. Lai, J. Liew, Design of steel fiber-reinforced high-strength concrete- encased steel short columns and beams, *ACI Structural Journal*, 2021, **118**, 45-59, doi: 10.14359/51728077.
[58] O. Ghodousian, R. Garcia, A. Ghodousian, M. H. Mohammad Nezhad Ayandeh, Properties of fibre-reinforced self-compacting concrete subjected to prolonged mixing: an experimental and fuzzy logic investigation, *Journal of Building Pathology and Rehabilitation*, 2024, **9**, 22, doi: 10.1007/s41024-023-00374-3.
[59] D. Sirimewan, N. Kunananthaseelan, S. N. Raman, R. Garcia, M. Arashpour, Optimizing waste handling with interactive AI: Prompt-guided segmentation of construction and demolition waste using computer vision, *Waste Management*, 2024, **190**, 149-160, doi: 10.1016/j.wasman.2024.09.018.
[60] C. Wattanapanich, T. Imjai, R. Sridhar, R. Garcia, B. S. Thomas, optimizing recycled aggregate concrete for severe conditions through machine learning techniques: a review, *Engineered Science*, 2024, **31**, 1191, doi: 10.30919/es1191.